

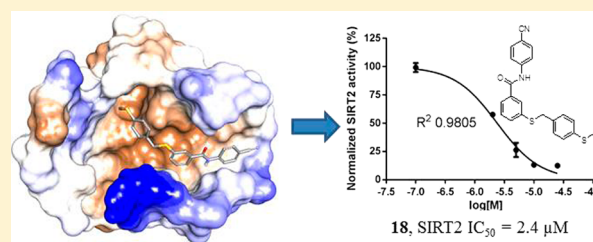
Design and Evaluation of 3-(Benzylthio)benzamide Derivatives as Potent and Selective SIRT2 Inhibitors

Mohammad A. Khanfar,^{†,‡} Luisa Quinti,[§] Hua Wang,[†] Johnathan Nobles,[§] Aleksey G. Kazantsev,^{*,§} and Richard B. Silverman^{*,†}[†]Department of Chemistry, Department of Molecular Biosciences, Chemistry of Life Processes Institute, Center for Molecular Innovation and Drug Discovery, Northwestern University, Evanston, Illinois 60208-3113, United States[‡]Department of Pharmaceutical Sciences, The University of Jordan, Amman, Jordan[§]Department of Neurology, Harvard Medical School and Massachusetts General Hospital, Charlestown, Massachusetts 02129-4404, United States

Supporting Information

ABSTRACT: Inhibitors of sirtuin-2 (SIRT2) deacetylase have been shown to be protective in various models of Huntington's disease (HD) by decreasing polyglutamine aggregation, a hallmark of HD pathology. The present study was directed at optimizing the potency of SIRT2 inhibitors containing the 3-(benzylsulfonamido)-benzamide scaffold and improving their metabolic stability. Molecular modeling and docking studies revealed an unfavorable role of the sulfonamide moiety for SIRT2 binding. This prompted us to replace the sulfonamide with thioether, sulfoxide, or sulfone groups. The thioether analogues were the most potent SIRT2 inhibitors with a two- to three-fold increase in potency relative to their corresponding sulfonamide analogues. The newly synthesized compounds also demonstrated higher SIRT2 selectivity over SIRT1 and SIRT3. Two thioether-derived compounds (17 and 18) increased α -tubulin acetylation in a dose-dependent manner in at least one neuronal cell line, and 18 was found to inhibit polyglutamine aggregation in PC12 cells.

KEYWORDS: SIRT2, Huntington's disease, docking, 3-(benzylthio)benzamide, polyglutamine aggregation



Human sirtuin-2 (SIRT2) belongs to the class III of histone deacetylases (HDAC), which require nicotinamide adenine dinucleotide (NAD⁺) for their function.^{1,2} SIRT2 has many known substrates, including α -tubulin,³ histones 3 and 4, transcription factors FOXO1 and FOXO3a, and others.⁴ SIRT2 is ubiquitously expressed in all tissues and highly abundant in the central nervous system (CNS). The expression of SIRT2 is significantly increased during neurodevelopment and remains strikingly high in the adult brain.³ Loss of SIRT2 through small-molecule inhibition or genetic ablation is beneficial for treatment of a number of neurodegenerative diseases. Pharmacological inhibition of SIRT2 increases neuronal survival in animal models of Parkinson's disease (PD), which is associated with changes in protein inclusion body characteristics.⁵ Moreover, SIRT2 inhibition mediates protection in neuronal and invertebrate models of Huntington's disease (HD), which is also associated with a reduction in polyglutamine (polyQ) aggregates, a hallmark of HD pathology.⁶

The efficacy of the sulfobenzoic acid derivative SIRT2 inhibitor, AK-1 (SIRT2 IC₅₀ = 12.5 μ M), in PD and HD models has been described (Figure 1).⁵⁻⁷ Brain-permeability of its close structural analogue, the selective SIRT2 inhibitor AK-7 (IC₅₀ = 15.5 μ M), has been reported.⁷ We have shown that treatment with AK-7 improved motor function, extended

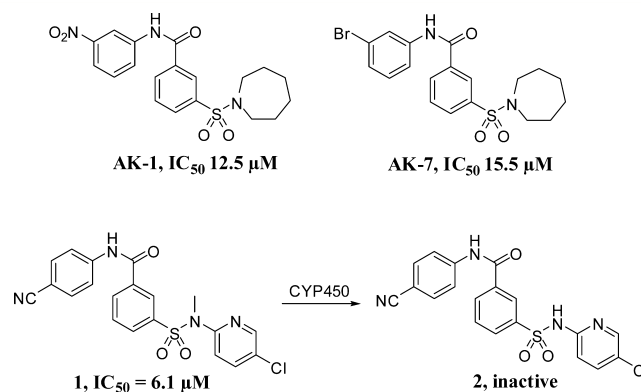


Figure 1. Structures of sulfobenzoic acid derivatives as SIRT2 inhibitors.

survival, reduced brain atrophy, and was associated with marked reduction of aggregated mutant huntingtin in two genetic mouse models of HD.⁸

Recently, we developed and characterized several 3-(benzylsulfonamido)benzamide derivatives as potent and

Received: February 15, 2015

Accepted: March 26, 2015

Published: March 26, 2015

selective SIRT2 inhibitors.⁹ Many of the synthesized compounds increased α -tubulin acetylation and inhibited polyQ aggregation in several neuronal cell lines.⁹ However, the reported compounds suffered from rapid metabolic oxidative demethylation at the sulfonamide nitrogen to the corresponding inactive metabolites (Figure 1).⁹

The inactivity of the demethylated analogues can be attributed to the hydrophilic properties of the sulfonamide group and, more decisively, to the formation of an acidic moiety, which can be partially ionized at physiological pH. For example, the calculated pK_a of demethylated analogue **2** using MarvinSketch is 6.7, which means that 83.4% (as calculated by the Henderson–Hasselbalch equation) of this compound is negatively charged and involved in electrostatically enforced hydrogen bonding interactions with water molecules, resulting in a high desolvation energy. Furthermore, analysis of the SIRT2 active site using the Discovery Studio suite revealed that the surface is highly hydrophobic (Figure 2A) and lacks any

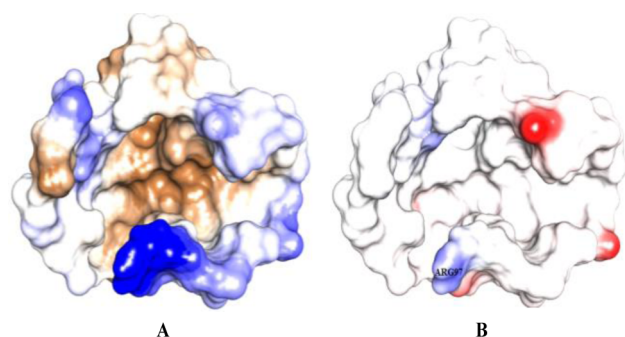


Figure 2. Surface of SIRT2 (pdb code 3ZGO) active site visualized by Discovery Studio suite. (A) Active site visualized by hydrophobicity; hydrophobic and hydrophilic amino acids are colored by brown and blue colors, respectively. (B) Active site visualized by ionizability; negatively and positively ionizable are colored in red and blue, respectively.

basic amino acids, except Arg97, which protrudes outside of the active site and is less likely to be involved in any ionic interaction with a bound ligand (Figure 2B). These results mean that the highly hydrophilic and possibly negatively charged sulfonamide moiety is not favorable, as it is not neutralized upon binding by an ionic interaction with a positively charged residue or incorporated in strong hydrogen bonding interactions inside the active site of SIRT2 to compensate for the high desolvation penalty of the sulfonamide moiety.

To further understand the binding interaction and orientation of 3-(benzylsulfonamido)benzamide derivatives within the SIRT2 active site, **2** was docked, in ionized and unionized states, in the active site of apo-SIRT2 (pdb code 3ZGO) using the LigandFit docking engine implemented in the Discovery Studio package.^{10,11} The SIRT2 active site was defined as described in the literature.^{12,13} Out of 100 poses generated by LigandFit, none of those with **2** in the ionized state was involved in an ionic interaction with Arg97. Moreover, in some of the docked poses the sulfonamide group formed one hydrogen bonding interaction, while it can form up to five hydrogen bonding interactions with water molecules in solution. Figure 3 shows the highest-ranked binding pose of **2** in the unionized form within the binding site of SIRT2. Clearly, the only moiety that participates in a hydrogen

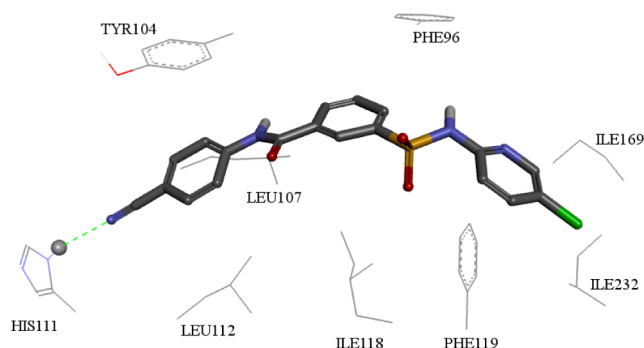


Figure 3. Highest ranked docked pose of demethylated analogue **2** within the active site of SIRT2 (pdb code 3ZGO). Side chains of the amino acids are only visualized for clarity.

bonding interaction is the cyano nitrogen with the imidazole group of His111. The sulfonamide group is surrounded by three hydrophobic amino acid residues; Phe96, Ile118, and Phe119. The 4-cyanophenyl moiety undergoes a hydrophobic interaction with Leu107 and Leu112 and has a sandwich-type π -stack with Tyr104. The chlorophenyl group is imbedded in the hydrophobic pocket of Ile169 and Ile232 and has a T-shaped π -stack with Phe119.

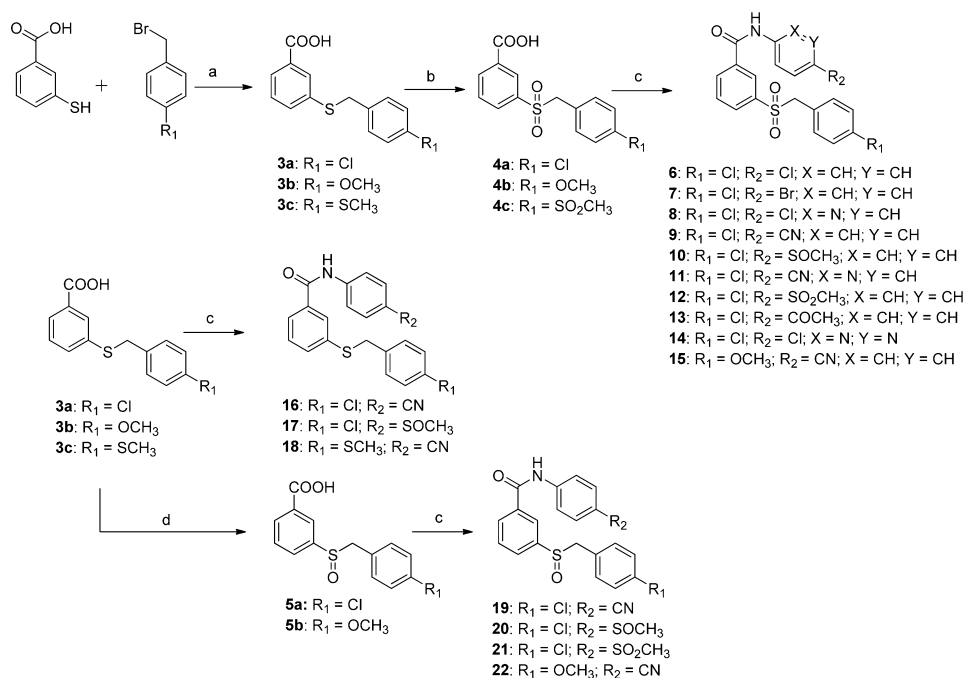
Similar docking results were obtained using a recent SIRT2 crystal structure with a cocrystallized inhibitor bound (pdb code 4RMH). The highest ranked docked pose shares interactions with amino acid residues similar to those identified with apo-SIRT2; however, the docked pose is inserted deeper within the active site inside the Phe143, Phe190, and Leu206 pocket, and the cyano group is hydrogen bonded to the amidic nitrogens of Phe243 and Phe235 (Figure S1 in Supporting Information).

These results add further confirmation to the unfavorable and insignificant role of the sulfonamide; however, *N*-methylation of the sulfonamide nitrogen can partially mask this effect and enhance ligand binding in a hydrophobic pocket.

In an attempt to overcome the metabolic inactivation and unfavorable role of the sulfonamide moiety, it was replaced by sulfone, sulfoxide, and thioether moieties, as shown in Scheme 1.

Commercially available 3-mercaptobenzoic acid and 3-benzyl bromide derivatives were coupled to yield 3-(benzylthio)-benzoic acid derivatives **3a–3c**, which were subjected to oxidation with excess H_2O_2 in acetic acid to generate the corresponding sulfones (**4a–4c**) or with one equivalent of H_2O_2 to form the sulfoxide intermediates (**5a and 5b**). Subsequently, the thioether, sulfoxide, and sulfone derivatives were coupled with aniline, pyridine, or pyridazine amines using EDCI and DMAP to form the final compounds (**6–22**); the sulfoxide chirality was not resolved.

Substituent selection was based on our previous work;⁹ those that showed high SIRT2 inhibitory activities were substituted at the para positions (R_1 and R_2 in Scheme 1) of the two phenyl rings. Therefore, chloro, methylthio, and methoxyl groups were added at the R_1 position, while cyano, halo, methylsulfinyl, and methylsulfonyl groups were added at the R_2 position. The potency and selectivity of the synthesized compounds were evaluated by applying robust, sensitive, and quantitative biochemical sirtuin deacetylation assays (SIRT1, **2**, **3**), as previously described.^{5,9} Compounds were screened at a single 10 μM dose in triplicate in the primary SIRT2 assay and counter-screened in SIRT1 and SIRT3 assays. **AK-1** was

Scheme 1. Synthetic Routes of Sulfone, Sulfoxide, and Thioether Derivatives^a

^aReagents and conditions: (a) (i) KOH, CH₃CH₂OH, H₂O, reflux, 2 h; (ii) 20% aq. NaOH, reflux, 1 h; (b) excess H₂O₂ (30%), 65 °C, 1 h; (c) Ar-NH₂, EDCI, DMAP, CH₂Cl₂; (d) H₂O₂ (30%, 1 equiv), 70 °C, 1 h.

included as a reference compound with each assay. Hits demonstrating higher or equal potency for SIRT2 inhibition compared to that of AK-1 were selected for dose–response studies, which were performed in multiple doses in the primary SIRT2 assay, including AK-1 for direct comparison.

These compounds also were subjected to SIRT1 and SIRT3 assays in multiple doses to determine sirtuin selectivity. The dose–response assays identified three analogues (9, 16, 18) as being more potent SIRT2 inhibitors than compound 1 (Table 1

Table 1. SIRT2 Activity and Selectivity of Sulfone, Sulfoxide, and Thioether Derivatives

compd no.	% of SIRT2 inhibition at 10 μM	IC ₅₀ (μM)	% SIRT1 inhibition at 10 μM	% SIRT3 inhibition at 10 μM
AK-1		12.5	10	5
1	67	6.1	10	8
6	0			
7	0			
8	2			
9	40	4.7	0	0
10	31			
11	36			
12	17			
13	23			
14	0			
15	50	6.7	3	0
16	81	2.9	8	0
17	60	8.4	10	8
18	83	2.4	3	0
19	47	7.1	12	11
20	24			
21	18			
22	21			

and Figure S2 in the Supporting Information), and six analogues (9, 15–19) as being more potent than AK-1. These inhibitors showed a high degree of selectivity, having weak SIRT1 and SIRT3 inhibition when tested at a concentration of 10 μM. The thioether analogues were the most potent and selective SIRT2 inhibitors, verifying the nonessential role of the sulfonamide moiety for SIRT2 binding. Furthermore, although the thioether moiety is known to undergo metabolic oxidation, it may not be detrimental because several sulfoxide and sulfone analogues were still active as SIRT2 inhibitors (e.g., 9, 15, 19). Other sulfoxide and sulfone analogues were less active (or inactive) than SIRT2 inhibitors. This might be a result of the high desolvation binding energy of analogues 10–14 and 20–22 within a highly hydrophobic active site or the absence of a hydrogen bond acceptor at the R₂ position for analogues 6–8 and 14. However, despite the metabolic oxidation potential, thioether (sulfoxide and sulfone) analogues are an improvement over the sulfonamides.

The dose–response curves of the tested compounds exhibited Hill slope values between –1 and –2, excellent correlation coefficients (Table S1 in Supporting Information), and low standard errors, which strongly suggest the authenticity (i.e., nonpromiscuity) of the SIRT2 inhibitors.¹⁴

To assess SIRT2 inhibition activity in live cells, we measured an increase in α-tubulin K40 acetylation, a known substrate for SIRT2 deacetylase, in neuronal rat ST14A¹⁵ and mouse Neuro2a cell lines. In this bioactivity test, extracts from cells treated with compounds for 6 h at a range of concentrations were resolved on SDS-PAGE and subjected to Western blot analysis using a primary antibody specific to acetylated lysine-40 of α-tubulin. Active SIRT2 inhibitors (9, 16–18) were tested, and two of them, 17 and 18, increased α-tubulin acetylation in a dose-dependent manner in at least one cell line. Figure 4A,B shows the bioactivity of SIRT2 inhibitors 18 and 17, respectively, after 6 h treatment in ST14A and Neuro2a

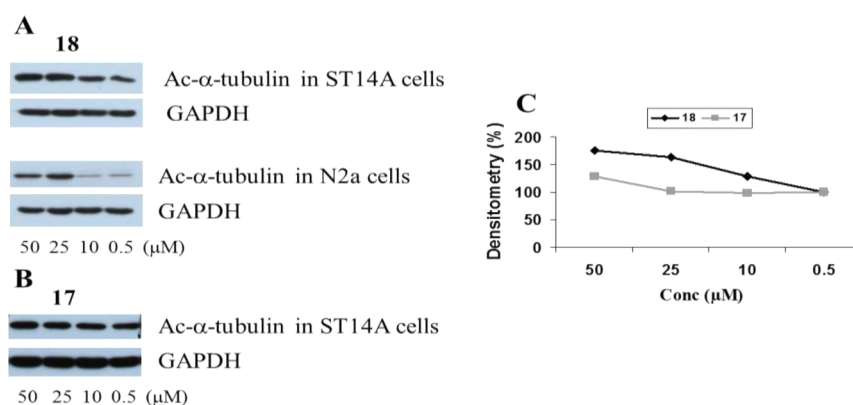


Figure 4. SIRT2 inhibitor effects on acetylation of α -tubulin K40. (A) Treatment of ST14A striatal cells and Neuro2a cells with **18** for 6 h resulted in an increase of α -tubulin acetylation as detected by immunoblotting; GAPDH is shown as a loading control. (B) Treatment of ST14A striatal cells with **17** for 6 h resulted in a weak increase of α -tubulin acetylation as detected by immunoblotting; GAPDH is shown as a loading control. (C) Compound dose-dependent increase of α -tubulin acetylation in ST14A striatal cells, normalized to GAPDH and quantified from Western blots in panels A and B.

cells at concentrations ranging from 0.5 to 50 μM . Compound **18** increased acetylation of α -tubulin in both neuronal cell lines (Figure 4A) and was found to be the most bioactive in this assay in a manner corresponding to its highest SIRT2 inhibition activity *in vitro*. Compound **17** showed weak activity against ST14A; however, it was inactive against Neuro2a cells. A comparison of **17** and **18** in ST14A cells is shown in Figure 4C.

Active SIRT2 inhibitor **18** was tested in a polyQ aggregation assay using rat neuronal PC12 cells expressing a short fragment of mutant huntingtin in an inducible fashion.^{16,17} The effect of **18** on polyQ aggregation was examined visually by fluorescence microscopy at doses of 25, 10, and 5 μM (Figure 5). Expression of the mutant huntingtin fragment was induced in PC12 cells simultaneously to compound treatment with 2.5 μM concentration of inducer muristerone A for 24 h, which

resulted in the formation of polyQ aggregates, visible in cells as large fluorescent inclusion bodies (Figure 5A). Inhibition of aggregation in this cell model can be detected as a reduction in the number and size of fluorescent polyQ inclusions. Analogue **18** was bioactive in this assay and significantly reduced the number and size of fluorescent polyQ inclusions (Figure 5B). A higher concentration (25 μM) of analogue **18** was required to shift the acetylation level in neuronal cell lines compared to the aggregation assay (5 μM). α -Tubulin is a very abundant protein, and a high concentration is required to observe a biological response.

In conclusion, starting with sulfonamide-derived compounds, we have been able to alter their structures to enhance potency and metabolic stability. We rationalized the insignificant role of the sulfonamide moiety in SIRT2 binding, which can be replaced by a thioether group. Several sulfone, sulfoxide, and thioether analogues were synthesized and tested for SIRT2 inhibitory activity and selectivity. The thioether analogues were the most potent and selective with a three-fold increase in potency. Two compounds (**17** and **18**) increased α -tubulin acetylation in a dose-dependent manner in at least one neuronal cell line. Additionally, active SIRT2 inhibitors were tested in a tertiary aggregation assay, and compound **18** was found to inhibit polyQ aggregation in PC12 cells. The results from this study are essential for further improvements of selective SIRT2 inhibitors.

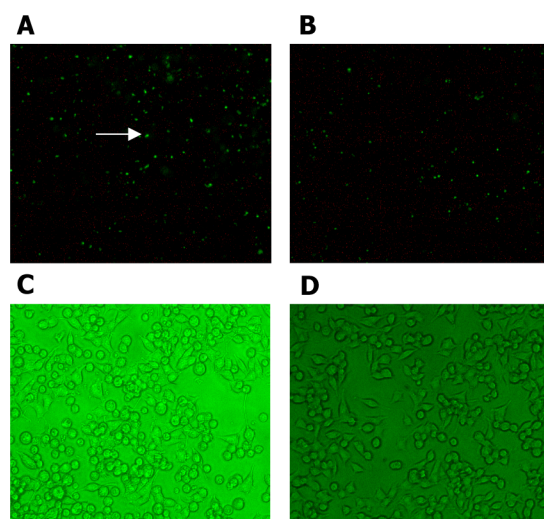


Figure 5. Effects of SIRT2 inhibitors on polyQ aggregation in PC12 cells. (A–D) Detection of aggregate inhibition using a microscopic epifluorescent assay. (A) Aggregation of extended polyQ peptides containing HD103Q-EGFP in PC12 cells induced with 2.5 μM muristerone for 24 h, which results in the formation of punctuated fluorescent inclusions (indicated by arrow). (B) Treatment with aggregation inhibitor **18** at 5 μM results in the reduction of fluorescent inclusion number and size. (C–D) Phase contrast cell images of panels A and B demonstrate equal cell density, i.e., lack of cytotoxicity.

■ ASSOCIATED CONTENT

Supporting Information

Analytical data of all compounds synthesized in this study and the experimental procedures. This material is available free of charge via the Internet at <http://pubs.acs.org>.

■ AUTHOR INFORMATION

Corresponding Authors

* (R.B.S.) Phone: 1-847-491-5653. Fax: 1-847-491-7713. E-mail: agman@chem.northwestern.edu.

* (A.G.K.) Phone: 1-617-726-1274. Fax: 617-724-1480. E-mail: akazantsev@mgh.harvard.edu.

Funding

The authors are grateful to the National Institutes of Health (Grant U01 NS066912) for financial support of this research.

Notes

The authors declare no competing financial interest.

■ ABBREVIATIONS

CNS, central nervous system; HD, Huntington's disease; HDAC, histone deacetylase; Parkinson's disease, PD; PolyQ, polyglutamine; SIRT2, sirtuin-2

■ REFERENCES

(1) Raghavan, A.; Shah, Z. A. Sirtuins in neurodegenerative diseases: a biological-chemical perspective. *Neurodegener. Dis* **2012**, *9*, 1–10.

(2) Schemies, J.; Uciechowska, U.; Sippl, W.; Jung, M. NAD(+)-dependent histone deacetylases (sirtuins) as novel therapeutic targets. *Med. Res. Rev.* **2010**, *30*, 861–889.

(3) North, B. J.; Marshall, B. L.; Borra, M. T.; Denu, J. M.; Verdin, E. The human Sir2 ortholog, SIRT2, is an NAD+-dependent tubulin deacetylase. *Mol. Cell* **2003**, *11*, 437–444.

(4) Taylor, D. M.; Maxwell, M. M.; Luthi-Carter, R.; Kazantsev, A. G. Biological and potential therapeutic roles of sirtuin deacetylases. *Cell. Mol. Life Sci.* **2008**, *65*, 4000–4018.

(5) Outeiro, T. F.; Kontopoulos, E.; Altmann, S. M.; Kufareva, I.; Strathearn, K. E.; Amore, A. M.; Volk, C. B.; Maxwell, M. M.; Rochet, J. C.; McLean, P. J.; Young, A. B.; Abagyan, R.; Feany, M. B.; Hyman, B. T.; Kazantsev, A. G. Sirtuin 2 inhibitors rescue alpha-synuclein-mediated toxicity in models of Parkinson's disease. *Science* **2007**, *317*, 516–519.

(6) Luthi-Carter, R.; Taylor, D. M.; Pallos, J.; Lambert, E.; Amore, A.; Parker, A.; Moffitt, H.; Smith, D. L.; Runne, H.; Gokce, O.; Kuhn, A.; Xiang, Z.; Maxwell, M. M.; Reeves, S. A.; Bates, G. P.; Neri, C.; Thompson, L. M.; Marsh, J. L.; Kazantsev, A. G. SIRT2 inhibition achieves neuroprotection by decreasing sterol biosynthesis. *Proc. Natl. Acad. Sci. U.S.A.* **2010**, *107*, 7927–7932.

(7) Taylor, D. M.; Balabadra, U.; Xiang, Z.; Woodman, B.; Meade, S.; Amore, A.; Maxwell, M. M.; Reeves, S.; Bates, G. P.; Luthi-Carter, R.; Lowden, P. A.; Kazantsev, A. G. A brain-permeable small molecule reduces neuronal cholesterol by inhibiting activity of sirtuin 2 deacetylase. *ACS Chem. Biol.* **2011**, *6*, 540–546.

(8) Chopra, V.; Quinti, L.; Kim, J.; Vollar, L.; Narayanan, K. L.; Edgerly, C.; Cipicchio, P. M.; Lauver, M. A.; Choi, S. H.; Silverman, R. B.; Ferrante, R. J.; Hersch, S.; Kazantsev, A. G. The sirtuin 2 inhibitor AK-7 is neuroprotective in Huntington's disease mouse models. *Cell Rep.* **2012**, *2*, 1492–1497.

(9) Khanfar, M. A.; Quinti, L.; Wang, H.; Choi, S. H.; Kazantsev, A. G.; Silverman, R. B. Development and characterization of 3-(benzylsulfonamido)benzamides as potent and selective SIRT2 inhibitors. *Eur. J. Med. Chem.* **2014**, *76*, 414–426.

(10) Khanfar, M. A.; AbuKhader, M. M.; Alqtaishat, S.; Taha, M. O. Pharmacophore modeling, homology modeling, and in silico screening reveal mammalian target of rapamycin inhibitory activities for sotalol, glyburide, metipranolol, sulfamethizole, glipizide, and pioglitazone. *J. Mol. Graphics Model.* **2013**, *42*, 39–49.

(11) Khanfar, M. A.; Taha, M. O. Elaborate ligand-based modeling coupled with multiple linear regression and k nearest neighbor QSAR analyses unveiled new nanomolar mTOR inhibitors. *J. Chem. Inf. Model.* **2013**, *53*, 2587–2612.

(12) Neugebauer, R. C.; Uciechowska, U.; Meier, R.; Hruby, H.; Valkov, V.; Verdin, E.; Sippl, W.; Jung, M. Structure-activity studies on splitomicin derivatives as sirtuin inhibitors and computational prediction of binding mode. *J. Med. Chem.* **2008**, *51*, 1203–1213.

(13) Kiviranta, P. H.; Salo, H. S.; Leppanen, J.; Rinne, V. M.; Kyrlyenko, S.; Kuusisto, E.; Suuronen, T.; Salminen, A.; Poso, A.; Lahtela-Kakkonen, M.; Wallen, E. A. Characterization of the binding properties of SIRT2 inhibitors with a N-(3-phenylpropenoyl)-glycine tryptamide backbone. *Bioorg. Med. Chem.* **2008**, *16*, 8054–8062.

(14) Shoichet, B. K. Interpreting steep dose-response curves in early inhibitor discovery. *J. Med. Chem.* **2006**, *49*, 7274–7277.

(15) Ehrlich, M. E.; Conti, L.; Toselli, M.; Taglietti, L.; Fiorillo, E.; Taglietti, V.; Ivkovic, S.; Guinea, B.; Tranberg, A.; Sipione, S.;

Rigamonti, D.; Cattaneo, E. ST14A cells have properties of a medium-size spiny neuron. *Exp. Neurol.* **2001**, *167*, 215–226.

(16) Kazantsev, A.; Preisinger, E.; Dranovsky, A.; Goldgaber, D.; Housman, D. Insoluble detergent-resistant aggregates form between pathological and nonpathological lengths of polyglutamine in mammalian cells. *Proc. Natl. Acad. Sci. U.S.A.* **1999**, *96*, 11404–11409.

(17) Apostol, B. L.; Kazantsev, A.; Raffioni, S.; Illes, K.; Pallos, J.; Bodai, L.; Slepko, N.; Bear, J. E.; Gertler, F. B.; Hersch, S.; Housman, D. E.; Marsh, J. L.; Thompson, L. M. A cell-based assay for aggregation inhibitors as therapeutics of polyglutamine-repeat disease and validation in *Drosophila*. *Proc. Natl. Acad. Sci. U.S.A.* **2003**, *100*, 5950–5955.